Journal of Applied Electrochemistry **31**: 759–765, 2001.

Formation of intermediates during methanol oxidation: A quantitative DEMS study[†]

H. WANG**, T. LÖFFLER and H. BALTRUSCHAT*
Institut für Physikalische und Theoretische Chemie, Universität Bonn, Römerstrasse 164, D-53117 Bonn
*(*author for correspondence)*
*(**On leave of absence from the Department of Chemistry, Beijing Normal University, Beijing 100875, People's Republic of China)*

Received 4 April 2000; accepted in revised form 18 September 2000

Key words: CO_2, DEMS, methanol, methylformate, Pt(1 1 1), Pt(3 3 2), Ru

Abstract

Current efficiencies for the formation of CO_2 during methanol oxidation at smooth polycrystalline platinum electrodes were determined by differential electrochemical mass spectrometry in a thin layer flow through cell. In all cases, the current efficiencies are below 60%; in particular, values as low as 16% were found in 0.1 M methanol solution at 0.6 V, which shows that a large amount of soluble intermediates (formaldehyde and/or formic acid) are formed. The extent to which these soluble intermediates are further oxidized to CO_2 depends on the diffusion conditions. For methanol oxidation a parallel oxidation path via CO_{ad} is also active. The influence of the surface crystal structure and, in particular, of steps was also studied. Step decoration by foreign metals allowed examination of the effect of cocatalytic metals on well defined model surfaces.

1. Introduction

Considerable effort has been made to elucidate the exact mechanism of methanol oxidation at Pt and Pt-like electrodes. In particular, the role of a parallel path mechanism has often been discussed, according to which oxidation does not only proceed via adsorbed CO, which acts both as intermediate and catalyst poison, but also via a 'parallel' path, in which only weakly adsorbed species play a role. Recently, two independent studies [1–3] involving a classical quantitative analysis of oxidation currents and coverage by CO seemed to show that oxidation occurs at potentials at which adsorbed CO is not yet oxidized. This was denied in a DEMS study, which showed that CO_2 can only be detected at potentials at which adsorbed CO is also oxidized [4]. Furthermore, in terms of quantitative evaluation these studies did not take into account the possible formation of other products or longer lived intermediates. Such species, in particular the formation of formaldehyde and formic acid, have already been postulated in the sixties on the basis of convection dependence of the oxidation current: the stronger the convection, the more intermediates are transported away from the electrode surface and not oxidized, resulting in a decrease in the current [5].

Recently, the formation of up to 30% of formaldehyde was detected fluorometrically [6]. Furthermore, several DEMS studies reported the formation of methylformate, and, at high methanol concentrations and high temperatures in a DMFC, the formation of methanoldimethylacetal [7]. Except for this last study, which was performed at 175 °C in a DMFC, in all previous studies quantitative evaluation was not attempted. Our present study therefore aims at a quantitative evaluation of byproducts like methylformate, and a quantitative correlation between the oxidation current and the CO_2 formed, resulting in values for the current efficiency.

We have previously shown that by decorating the steps of stepped vicinal Pt(1 1 1) electrodes interesting model surfaces for bimetallic catalyst are obtained with a known atomic distance between the components [8, 9]. Therefore, we also present first results on current efficiencies and catalytic activities obtained with such surfaces, as well as the effect of surface structure on the current efficiency. The effect of surface crystal structure on the catalytic activity has been demonstrated previously [10–13].

2. Experimental details

A new thin layer cell, the dual thin layer flow-through cell made of titanium, was used for DEMS in combination with a Balzers quadrupole mass spectrometer

[†] Paper presented at the workshop on "Electrocatalysis in direct and indirect methanol fuel cells" held at Portoroz, Slovenia, September 1999.

(QMG 511). The construction of this cell was like that of the early cell made of Kel-F, described previously [14], but both compartments were connected via six capillaries of 0.5 mm diameter. The area of the working electrode was 0.28 cm^2, the roughness factor of the polycrystalline Pt electrode was 1.8.

All solutions were prepared with Millipore water. 0.5 M H_2SO_4 p.a. was used as supporting electrolyte. Methanol was spectropure grade. The solutions were deaerated with argon.

Prior to each experiment, the electrode was cleaned in 0.5 M H_2SO_4 by cycling between 0.05 and 1.5 V at a scan rate of 50 mV s^{-1}. The potential was then stopped at 0.05 V and the base electrolyte was replaced by the solution containing methanol. Then a positive potential sweep was resumed at a scan rate of 10 mV s^{-1}, at the same time the mass intensity for $m/z = 44$ (most intensive ion of CO_2) was measured. After the first cycle a stable voltammogram was obtained, except the Pt(3 3 2) decorated with Sn or Ru, where the current increased somewhat up to the sixth sweep. In potential step experiments, the starting potential was also 0.05 V, that is, a potential at which methanol does not adsorb at Pt.

An average value for the current efficiency was obtained by integrating CV and MSCV from 0.45 to 1.50 V and then back to 0.45 V. The faradaic charge, Q_f, and the integrated ion current, $Q_i(44)$, were thus obtained. That part of the charge which corresponds to the formation of CO_2 (the faradaic charge) was obtained by Equation 1:

$$Q_f^* = 6\,Q_i(44)/K^*(44) \tag{1}$$

where Q_f^* is the faradaic charge corresponding to the formation of CO_2 in a cycle of the potential sweep, $Q_i(44)$ is the integrated ion current for CO_2 in a cycle of the potential sweep, 6 is the number of electrons for methanol oxidation to CO_2, and $K^*(44)$ is the calibration constant, which is determined from a calibration experiment involving CO oxidation, as described in [15].

Then, the current efficiency for CO_2 was determined by Equation 2:

$$A_q = Q_f^*/Q_f \tag{2}$$

where A_q is the average current efficiency for CO_2 in a cycle of potential sweep, and Q_f is the faradaic charge in a cycle of potential sweep.

Similarly, the current efficiency for CO_2 can also be determined from the faradaic current, I_f, and ion current, I_i.

$$I_f^* = 6\,I_i(44)/K^*(44) \tag{3}$$

$$A_i = I_f^*/I_f \tag{4}$$

where I_f^* is faradaic current corresponding to the formation of CO_2, I_f is faradaic current, $I_i(44)$ is ion current for CO_2 and A_i is current efficiency for CO_2.

In the potential step experiments the faradaic current and mass intensity values one minute after the potential was stepped were used for evaluation.

As we will show in a forthcoming paper, incomplete mixing of the electrolyte in the capillaries between the outlet of the electrochemical thin layer cell and the entrance of the detection cell occurs at higher flow rates (5 μL s^{-1} and above) and largely influences the transfer efficiency. Therefore, calibration for CO_2 was performed for each flow value separately (the calibration constant K^* includes the transfer efficiency N according to $K^* = NK^0/F$).

The calibration constant K^0 for methylformate was determined by the corresponding ion current during a known gas flow into the mass spectrometer, the same water pressure as in electrochemical experiments was adjusted by connecting the electrochemical cell during the calibration experiment. From this, K^* for methylformate was calculated using the transfer efficiency for CO_2 and correcting it for the difference in collection efficiencies between CO_2 and methylformate in the detection compartment (the ratio of collection efficiencies is 1 at 1 μL s^{-1} and about 2 at 5 μL s^{-1}).

Since the transport of methanol from the solution phase to the gas phase is not diffusion limited [16], such a correction is not possible. Therefore, for low flow rates, when mixing in the capillaries is complete (1 μL s^{-1}), that is, a homogeneous concentration is achieved before the entrance of the detection cell, calibration was simply achieved from the ion current at the low potential limit of the cyclic voltammograms, where no reaction occurs. We verified, that the ion current is proportional to the methanol concentration. At higher flow rate mixing is incomplete, and the ion current does not reflect the average concentration of the solution entering the detection cell. Therefore, the amount of consumed methanol was only determined at the flow rate of 1 μL s^{-1}.

Small coverages of Ru and Sn were achieved as follows: Ru was deposited at 0.6 V vs RHE for 5 min from 5×10^{-3} M $RuCl_3$ in 0.1 M H_2SO_4. Sn was deposited at 0.6 V vs RHE for 3 min from 1×10^{-4} M $SnSO_4$ in 0.5 M H_2SO_4. Both depositions were carried out in separate cells and resulted in coverages of 0.25 for Ru on Pt(1 1 1) and Pt(3 3 2) and 0.63 or 0.26 for Sn on Pt(1 1 1) and Pt(3 3 2), respectively [17]. Details of the deposition procedure are given in [8, 9].

3. Results

Cyclic voltammograms for methanol oxidation and the corresponding mass spectrometric cyclic voltammograms for $m/z = 44$ (CO_2) and $m/z = 60$ (methylformate) are shown in Figures 1 and 2 for two different concentrations. In the first sweep the hydrogen adsorption peak is still visible, showing that methanol does not yet adsorb at the potential where methanol is introduced into the cell. The shoulder at 0.5 V is not caused by the

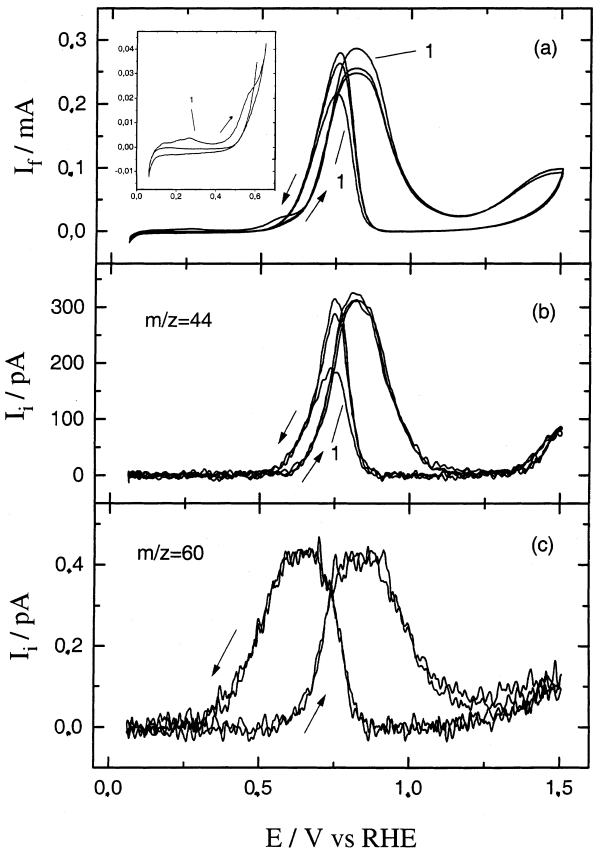

Fig. 1. Simultaneously recorded CV (a), MSCV $m/z = 44$ (b) and MSCV $m/z = 60$ (c) on polycrystalline platinum in 0.1 M methanol + 0.5 M H_2SO_4 solution. Scan rate 10 mV s^{-1}. Electrolyte flow rate 5 μL s^{-1}. 3 cycles shown. (Inset: expanded view of the faradaic current in the low potential range. Number '1' in Figure indicates first cycle. Arrows indicate direction of potential sweep.)

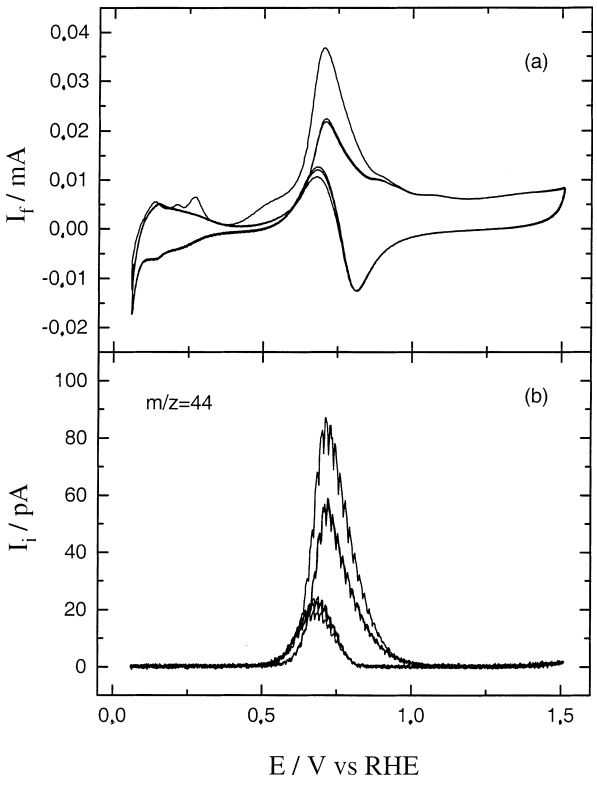

Fig. 2. Simultaneously recorded CV (a), MSCV $m/z = 44$ (b) on polycrystalline platinum in 0.001 M methanol + 0.5 M H_2SO_4 solution. Scan rate 10 mV s^{-1}. Electrolyte flow rate 5 μL s^{-1}. Three cycles are shown.

formation of CO_2. It is due to the adsorption of methanol according to $CH_3OH \rightarrow CO_{ad} + 4\,H^+ + 4\,e^-$ [4]. Formation of methylformate was below the detection limit at the lower methanol concentration.

Table 1 gives the current efficiencies for CO_2 for three different methanol concentrations and three different flow rates. In all cases it is below 50%, which demonstrates the importance of other products. The current efficiency decreases with increasing flow rate and increasing concentration. This supports the parallel path mechanism, according to which formaldehyde and/or formic acid are formed; the higher the flow rate, the more of the intermediates are transported away from the electrode without reaction. Diffusion and convection is therefore competing with their oxidation (cf. the reaction scheme below).

Typical potential step experiments are shown in Figures 3 and 4. The corresponding yields are summarised in Table 2 for different step potentials. Particularly interesting is the fact that, at low oxidation potentials in 0.1 M methanol solution, the current efficiency for CO_2 of 16 to 18% is independent of the flow rate. Besides CO_2, methylformate was also detected in 0.1 M methanol solution at 0.6 V. A quantitative analysis of the ionic current (or ionic charge) showed that its amount is up to 10 or 20% that of CO_2 formed.

Unfortunately, other products like formaldehyde and formic acid are not volatile enough to be detected by

Table 1. Effect of methanol concentration and electrolyte flow rate on methanol oxidation
C concentration of methanol in 0.5 M H_2SO_4; *u* flow rate of the solution; A_q average current efficiency for CO_2; n_3 amount of CO_2; n_4 amount of $HCOOCH_3$; *z* number of consumed electrons per methanol molecule; and 'n.d' no signal for $m/z = 60$ is detectable.

C /mol L^{-1}	u /μL s^{-1}	Q_f /mC	$Q_i(44)$ /C	$K^*(44)$	A_q	n_3/n_4	z
0.001	1.1	0.87	1.7×10^{-9}	2.6×10^{-5}	46%	n.d.	4.65
0.001	5	0.87	1.3×10^{-9}	2.0×10^{-5}	43%	n.d.	
0.001	10	0.87	1.0×10^{-9}	1.9×10^{-5}	38%	n.d.	
0.01	1.1	3.96	6.5×10^{-9}	2.6×10^{-5}	38%	n.d.	3.87
0.01	5	3.95	4.6×10^{-9}	2.0×10^{-5}	35%	n.d.	
0.01	10	4.02	4.0×10^{-9}	1.9×10^{-5}	32%	n.d.	
0.1	1.1	15.2	1.9×10^{-8}	2.5×10^{-5}	30%	54	2.64
0.1	5	14.2	1.3×10^{-8}	1.9×10^{-5}	28%	40	

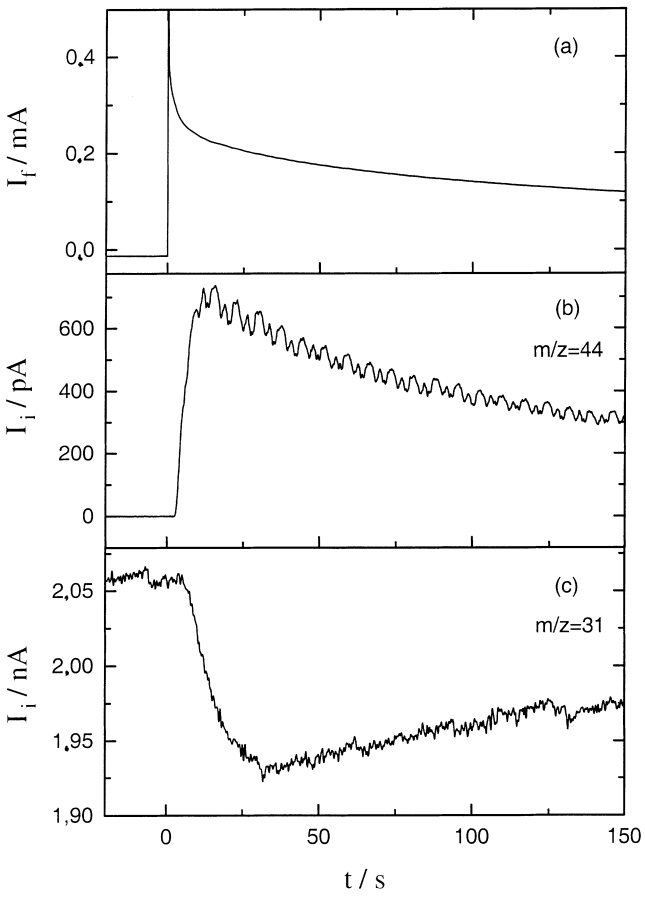

Fig. 3. Simultaneously recorded transients of faradaic current (a) and ion current $m/z = 44$ (b) and $m/z = 31$ (c) on polycrystalline platinum in 0.01 M methanol + 0.5 M H_2SO_4 solution after the step of potential from 0.05 to 0.75 V. Electrolyte flow rate 1.1 μL s^{-1}.

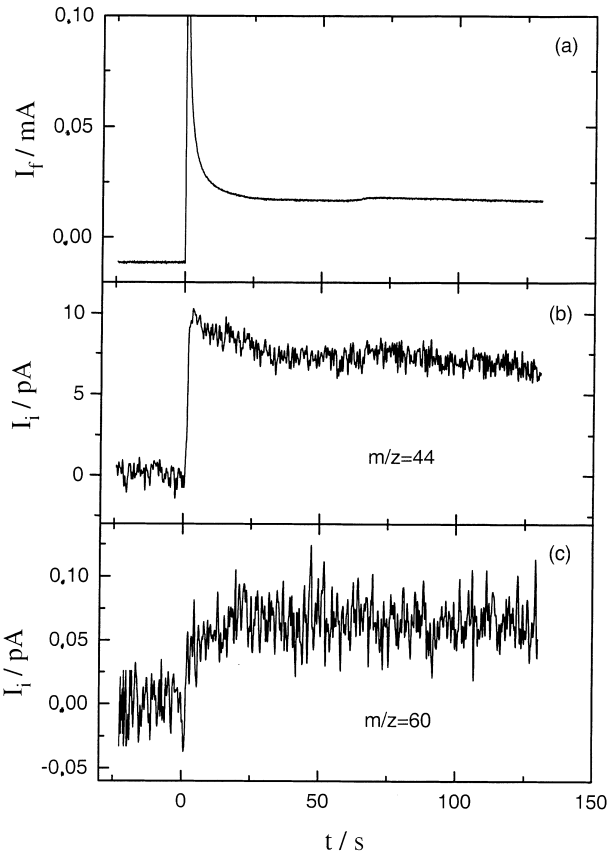

Fig. 4. Simultaneously recorded transients of faradaic current (a) and ion current $m/z = 44$ (b) and $m/z = 60$ (c) on polycrystalline platinum in 0.1 M methanol + 0.5 M H_2SO_4 solution after the step of potential from 0.05 to 0.6 V. Electrolyte flow rate 5 μL s^{-1}.

DEMS. We therefore tried to get indirect information on such products by quantifying the amount of methanol consumed and calculating the number of electrons per methanol molecule (cf. Figure 3(c)). From the amount or rate of methanol consumption (Δx), the amount or rate of produced CO_2 (x_3) and the faradaic current, I_f, the amount or rate of formaldehyde (x_1) and formic acid (x_2) production can be calculated using Equation 5 for charge balance and Equation 6 for mass balance:

$$I_f/F = 2x_1 + 4x_2 + 6x_3 \quad (5)$$

$$\Delta x = x_1 + x_2 + x_3 \quad (6)$$

where F is the faradaic constant (96 500 C mol^{-1}).

For the conditions of Table 2 and a flow rate of 1.1 μL s^{-1}, the yields of formaldehyde, formic acid and CO_2 are thus

Table 2. The current efficiency for CO_2 one minute after the potential-step from 0.05 V to E_{step}
C concentration of methanol in 0.5 M H_2SO_4; u flow rate of the solution; A_i current efficiency for CO_2; x_3 formation rate of CO_2; x_4 formation rate of $HCOOCH_3$; z number of consumed electrons per methanol molecule; and 'n.d.' no signal for $m/z = 60$ is detectable.

C /mol L^{-1}	u /μL s^{-1}	$E^{\dagger}_{step}$ /V	I_f /mA	$I_i(44)$ /A	$K^*(44)$	A_i	x_3/x_4	z
0.001	1.1	0.65	0.023	7.5×10^{-11}	3.4×10^{-5}	57%	n.d.	3.6
0.001	5	0.65	0.021	5.1×10^{-11}	2.6×10^{-5}	57%	n.d.	
0.001	10	0.65	0.021	4.5×10^{-11}	2.4×10^{-5}	55%	n.d.	
0.01	1.1	0.65	0.038	6.2×10^{-11}	3.4×10^{-5}	29%	n.d.	3.3
0.01	1.1	0.75	0.16	4.5×10^{-10}	3.4×10^{-5}	49%	n.d.	3.0
0.1	1.9	0.6	0.020	1.3×10^{-11}	2.1×10^{-5}	18%	8.6	
0.1	5	0.6	0.018	6.8×10^{-12}	1.3×10^{-5}	18%	10	
0.1	8.3	0.6	0.019	7.9×10^{-12}	1.6×10^{-5}	16%	5.7	

$^{\dagger}E_{step}$ potentials are measured with reference to RHE.

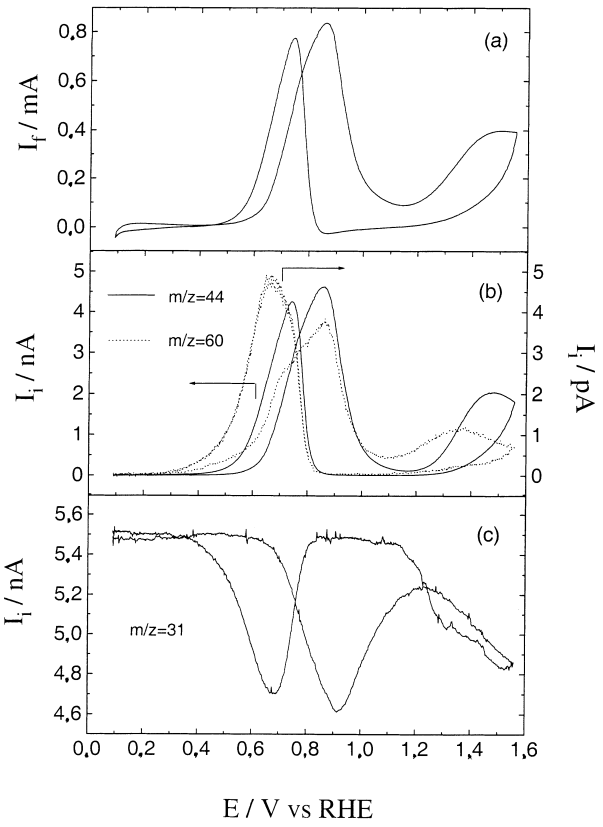

Fig. 5. Simultaneously recorded CV (a), MSCVs $m/z = 44$ and $m/z = 60$ (b) and MSCV $m/z = 31$ (c) on platinum sputtered on Teflon in 0.1 M methanol + 0.5 M H_2SO_4 solution in the conventional cell. Scan rate 10 mV s^{-1}. Methanol electrolyte was stirred with strong Ar stream.

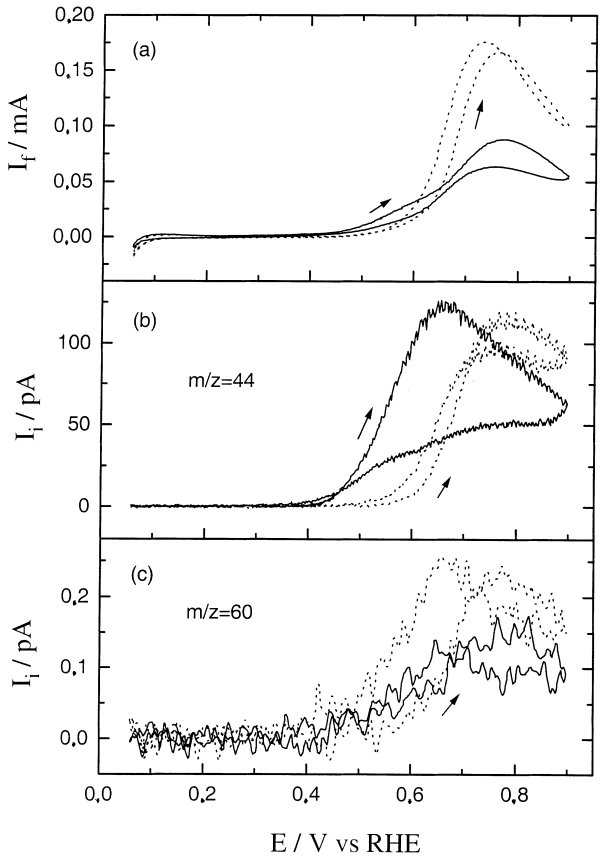

Fig. 6. Simultaneously recorded CV (a), MSCVs $m/z = 44$ (b) and MSCVs $m/z = 60$ (c) on Pt(3 3 2) (·····) and Pt(3 3 2)-Ru (—) in 0.1 M methanol + 0.5 M H_2SO_4 solution. Scan rate 10 mV s^{-1}. Electrolyte flow rate 5 μL s^{-1}.

56%, 10% and 34% at 0.65 V and $C_{Meth} = 1$ m M

50%, 34% and 16% at 0.65 V and $C_{Meth} = 10$ m M

72%, 3% and 25% at 0.75 V and $C_{Meth} = 10$ m M

For comparison, we also determined the current efficiencies on rough, sputtered Pt electrodes in a conventional DEMS cell (Figure 5). Identical results were obtained when using 0.1 M $HClO_4$ instead of 0.5 M H_2SO_4 as supporting electrolyte. Due to the higher amounts of species formed at this rough electrode, it can be clearly seen that the production of the methylformate starts at lower potential than that of CO_2. The current efficiency is high (90%) because intermediates stay close to the electrode (no convection) and are subsequently oxidized. Here, a quantification of the amount of methanol consumed is not possible due to the ill-defined convection and diffusion. The ionic current for $m/z = 60$ changes very little from 0.65 to 0.75 V. This also suggests that the relative contribution of formic acid decreases from 0.65 to 0.75 V, as stated above.

The flow through cell also allows measurement of the production of CO_2 at single crystal electrodes. As an example, this is shown for Pt(3 3 2) and Pt(3 3 2) with steps decorated by Ru in Figure 6. Average current efficiencies for clean Pt(1 1 1) and Pt(3 3 2) surfaces, as well as for surfaces modified by cocatalyst (Ru and Sn), are given in Table 3. The highest current efficiency is observed for Pt(3 3 2) modified by Ru, although the peak current, as well as the total charge during one cycle, are decreased. Modification of the surface by Sn only has a small effect. The lowest current efficiency, as well as the lowest peak current, is observed for the smooth Pt(1 1 1) surface.

4. Discussion

The low values of the current efficiencies, and in particular their decrease with increasing flow rate, shows that methanol oxidation proceeds predominantly via dissolved intermediates, which are able to diffuse away from the electrode surface under forced convection. Potential step experiments have shown that, at high concentrations and low potentials, a limiting value of 16% is reached, which is independent of the flow rate. This is an indication that this value corresponds to the amount of CO_2 formed through the oxidation path not involving dissolved intermediates (i.e., via adsorbed CO).

This shows the validity of the parallel path mechanism according to the following scheme:

Table 3. Methanol electrooxidation on different Pt electrodes (electrolyte flow rate $u = 5\ \mu L\ s^{-1}$, methanol concentration 0.1 M) Data evaluation used 2nd or subsequent sweep.

	E^{max} /V	I_f^{max} /mA	$I_i^{max}(44)$ /10^{-10}A	$I_i^{max}(60)$ /10^{-13}A	Q_f /mC	A_i^{max}	A_q	n^{44}/n^{60} (max)	n^{44}/n^{60} (total)	I_f /mA at 0.65 V	A_i at 0.65 V
Pt(3 3 2)	0.76	0.17	1.1	2.3	7.6	28%	27%	49	37	0.042	35%
Pt(3 3 2)-r	0.77	0.36	2.2	5.1	16	25%	23%	42	30	0.089	18%
Pt(3 3 2)-Ru	0.77	0.091	0.94	1.5	4.1	35%	46%	63	71	0.044	96%
Pt(3 3 2)-Sn	0.80	0.10	0.86	2.0	3.0	24%	23%	43	30	0.033	27%
Pt(1 1 1)	0.79	0.027	0.19	0.53	1.2	18%	20%	35	28	0.0077	45%
Pt(1 1 1)-r	0.78	0.56	6.3	14	23	30%	27%	46	33	0.094	19%
Poly-Pt	0.82	0.25	3.1	4.2	14	39%	28%	74	40	0.039	21%

n^{44}/n^{60} refers to the ratio of the amount of CO_2 and methylformate; 'max' refers to the potential of the maximum of faradaic current; 'total' refers to a cycle of potential sweep; and 'r' means the roughened surface.

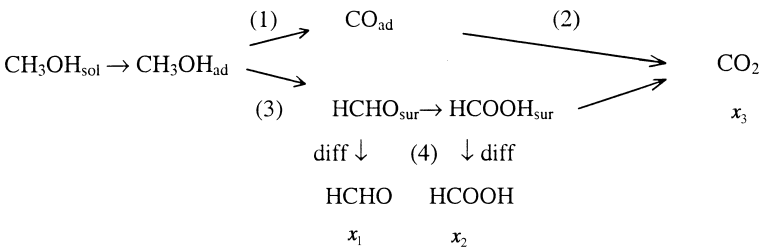

The finding that the current efficiency is lower for lower oxidation potentials (Table 2) is paralleled by the observation that the relative contribution of methylformate is higher at lower potentials (cf. Figure 5). Methylformate is presumably formed in a subsequent reaction from formic acid and methanol. Therefore, the reaction path via Reactions 3 and 4 predominates at lower potentials. On the basis of IR measurements, it was suggested [10] that methylformate is formed directly on the electrode surface and not in a subsequent reaction in solution. Since ester formation reactions are very slow (time constant in the range of hours [18]), and a concentration of 0.2 μM methylformate is estimated from the data of Table 2, which is close to the equilibrium concentration, it is probable that the ester formation is catalysed by the electrode surface.

The formation of formaldehyde and formic acid seems to be contradictory to the well known observation that oxidation of these molecules is faster than that of methanol. However, this refers to equal concentrations, whereas increased diffusion due to forced convection leads to a very low concentration of these species in the vicinity of the electrode. Whether the formation of those intermediates plays a role in fuel cells depends on the actual diffusion conditions and, of course, on the temperature dependence of the relative importance of the two reaction paths. The observed formation of methylformate and methanaldimethylacetate in a DMFC [7] points to the importance of formic acid and formaldehyde.

Best suited for a comparison of the catalytic activity of the different modified and unmodified single crystal surfaces is the current and the current efficiency at a given potential. We chose 0.65 V in Table 3, because this potential is below the current maximum and still leads to reasonable current densities for all surfaces studied. It is interesting to note that the surface with the higher current density, that is, the apparently higher catalytic activity (roughened Pt(3 3 2)), is that with the lower current efficiency. On the other hand, for the surface with the highest current efficiency (Ru modified Pt(3 3 2), a fairly low current density is observed. In contrast to the case of pure Pt, the maximum of the formation rate of methylformate is achieved at more positive potentials than that of CO_2 (cf. Figure 5). This confirms the observation that the current efficiency is higher at lower potentials above 90% at 0.65 V vs 35% at the potential of the current maximum (i.e., 0.75 V). The data obtained from cyclic voltammograms (i.e., under nonsteady conditions) have to be interpreted with some care, because they are influenced by the oxidation of adsorbed CO. Whereas for the Ru modified surface adsorbed CO only amounts to around 20% of the CO_2 formed, this is a particular problem for the Pt(1 1 1) surface with the low oxidation current. It is clear that for a detailed analysis, steady reaction rates have to be known as obtained in potential step experiments. Such measurements are also in progress for single crystalline and modified surfaces.

It has been claimed that the best surface composition of Pt–Ru alloys for methanol oxidation is 10% Ru [19]. On the other hand, in actual direct methanol fuel cells catalysts with a Ru content of 50% are usually used [20]. This discrepancy may be due to different temperatures, but also a different reason is possible: in fundamental studies at smooth electrodes, the catalytic activity is judged from the current density. On the other hand, in a

fuel cell, all the fuel has to be consumed and the diffusion conditions are quite different.

5. Conclusions

Oxidation of methanol proceeds via a parallel path mechanism indeed. One oxidation path is via adsorbed CO and the other occurs via dissolved intermediates (formaldehyde and formic acid). The relative contribution of the two paths depends on several factors:

(i) At high flow rate, the more soluble intermediates are transported away from the electrode without further reaction to CO_2; therefore the current efficiency decreases.

(ii) At more positive potentials, methanol oxidation via CO_{ad} is promoted due to the faster oxidation of CO_{ad}. The reaction via soluble intermediates is less dependent on potential; therefore the current efficiency increases.

(iii) Whereas the rate of oxidation via CO_{ad} is largely limited by the oxidation rate of CO_{ad} (in particular at lower potentials), which is independent of methanol concentration, the rate of methanol oxidation via dissolved intermediates increases with the increase of methanol concentration. Therefore, the current efficiency decreases with increasing methanol concentration.

At electrodes with porous structures, such as used in fuel cells, the reaction of these intermediates is faster than their diffusion. Nevertheless, they will be formed to some extent and alter the composition of the fuel during the start-up of a fuel cell system.

Ru as a catalyst component not only acts by lowering the oxidation potential of the poisoning adsorbed CO, but also by increasing the current efficiency. A possible explanation is that the fast oxidation of adsorbed CO induces a shift from the reaction path via soluble intermediates to that via adsorbed CO. Another possible explanation is that Ru promotes the oxidation of soluble intermediates to CO_2. Further studies are in progress to distinguish between these two possibilities.

Acknowledgement

Thanks are due to the DFG for financial support. H. Wang is grateful to the Hanns-Seidel-Stiftung for a stipend.

References

1. E. Herrero, K. Franaszczuk and A. Wieckowski, *J. Phys. Chem.* **98** (1994) 5074.
2. E. Herrero, W. Chrzanowski and A. Wieckowski, *J. Phys. Chem.* **99** (1995) 10423.
3. T.D. Jarvi and E.M. Stuve, 'Fundamental Aspects of Vacuum and Electrocatalytic Reactions of Methanol and Formic Acid on Platinum Surfaces, *in* J. Lipkowski and P.N. Ross (Eds.), 'Electrocatalysis' (Wiley-VCH, New York, 1998), p. 75.
4. W. Vielstich and X.H. Xia, *J. Phys. Chem.* **99** (1995) 10421.
5. W. Vielstich, 'Fuel Cells. Modern Processes for the Electrochemical Production of Energy' (Wiley-Interscience, London New York, 1965).
6. C. Korzeniewski and C. Childers, *J. Phys. Chem. B* **102** (1998) 489.
7. S. Wasmus, J.-T. Wang and R.F. Savinell, *J. Electrochem. Soc.* **142** (1995) 3825.
8. P. Berenz, S. Tillmann, H. Massong and H. Baltruschat, *Electrochim. Acta* **43** (1998) 3035.
9. H. Massong, S. Tillmann, T. Langkau, E.A. Abd El Meguid and H. Baltruschat, *Electrochim. Acta* **44** (1998) 1379.
10. J. Shin and C. Korzeniewski, *J. Phys. Chem.* **99** (1995) 3419.
11. C. Lamy, J.M. Leger, J. Clavilier and R. Parsons, *J. Electroanal. Chem.* **150** (1983) 71.
12. X.H. Xia, T. Iwasita, F. Ge and W. Vielstich, *Electrochim. Acta* **41** (1996) 711.
13. E. Herrero, K. Franaszczuk and A. Wieckowski, *J. Phys. Chem.* **98** (1994) 5074.
14. Z. Jusys, H. Massong and H. Baltruschat, *J. Electrochem. Soc.* **146** (1999) 1093.
15. H. Baltruschat and U. Schmiemann, *Ber. Bunsenges. Phys. Chem.* **97** (1993) 452.
16. H. Baltruschat, Differential electrochemical mass spectrometry as a tool for interfacial studies, *in* A. Wieckowski (Ed.), 'Interfacial Electrochemistry' (Marcel Dekker, New York, 1999), p. 577.
17. H. Massong, H. Wang, G. Samjeské and H. Baltruschat, *Electrochim. Acta* **46** (2000) 701.
18. D.R. Storm and J.D.E. Koshland, *J. Am. Chem. Soc.* **94** (1972) 5805.
19. H.A. Gasteiger, N. Markovic, P.N. Ross and E.J. Cairns, *J. Phys. Chem.* **97** (1993) 12020.
20. X. Ren, M.S. Wilson and S. Gottesfeld, *J. Electrochem. Soc.* **143** (1996) L12.